

Experimental investigation of formability of woven textile composite preform in stamping operation

B. Zhu¹, T.X. Yu¹, H. Zhang², X.M. Tao²

¹*Department of Mechanical Engineering, HKUST, Clear Water Bay, Kowloon, Hong Kong*
URL: www.ust.hk e-mail: mezab@alumni.ust.hk; metxyu@ust.hk

²*Institute of Textiles and Clothing, Hong Kong PolyU, Hung Hom, Kowloon, Hong Kong*
URL: www.polyu.edu.hk e-mail: tctaoxm@inet.polyu.edu.hk

ABSTRACT: This paper presents experimental stamping operation on woven textile composite preform made of commingled E-glass fibers reinforced Polypropylene (PP) with strain measurement by conductive fiber sensors. A series of stamping tests are implemented in the university lab at room temperature, from which a previously proposed theoretical criterion of wrinkling is validated. Through the measured shear distribution and evolution, the deformation behaviour of textile fabric is found to be a result of cooperation of both mould shape and initial sample orientation, helping to build up a simplified model of the composite sheets during their hot forming process. Finally, the stamping parameters were optimized according to the experimental and theoretical work.

Key words: Woven textile composite, Stamping, Formability, Failure

1 INTRODUCTION

Textile composites, used as structural components, have attracted lots of academic attention due to their superiorities compared with conventional metals and laminates. In the industry, the most efficient way to form the material is through stamping operation, where a flat sheet is stamped into a particular shape with a pair of punch and die at a high temperature. Stamping is a very cheap process with a cycle of only seconds regardless of the size of the parts. It can reduce the cycle time by several times in comparison with some other methods of forming complex structural composite products with medium volume. However, material's formability remains as a challenging issue, which is restricted by failure mechanisms such as wrinkling and slippage.

Many researchers have conducted experimental, numerical and theoretical work to investigate the formability of material in stamping operation [1-3]. Previous studies have indicated that the sheet formability is governed by the complex interplay between pure stretch forming and pure deep drawing, which is relevant to the tool profile, blank size and

blank-holder force [4]. As for the failure of wrinkling, several researchers have carried out experimental measurements and proposed analytical models [5,6]. In particular, a theoretical criterion has been established involving all key textile parameters and material properties [7], which will be evaluated in the present paper so as to investigate material's formability and optimize the stamping conditions.

2 CONDUCTIVE FIBER SENSOR

Large strain and high temperature are two very common conditions in the formation of fabric reinforcement polymer resin composites in stamping processes. Polyacrylonitrile (PAN) based stable carbon filament yarn with a carbonized temperature of 1000°C was designed and fabricated in a single warp chain of weft-plain-knitted fabric by the Institute of Textiles and Clothing, HKPolyU [8]. The sensor was calibrated in both simple tension and shear test at various temperatures and loading speeds, indicating a good stability and repeatability within a strain measuring range of 10%.

3 STAMPING TEST

3.1 Measurement by conductive fiber sensors

The stamping was implemented on an equipment of eccentric cone mould under a constant stamping speed of 200mm/min at room temperature, as shown in figure 1(a). The specimen was the same as described in the previous paper [7]. A uniform circular distribution of dead weight with 10kg×8 around the edge of die was used as the blank holder force. The specimen was initially orientated that the diagonal line between two sets of yarn was along the largest slope direction of the mould contour. The equipment was connected with the UTM with displacement control of the punch.

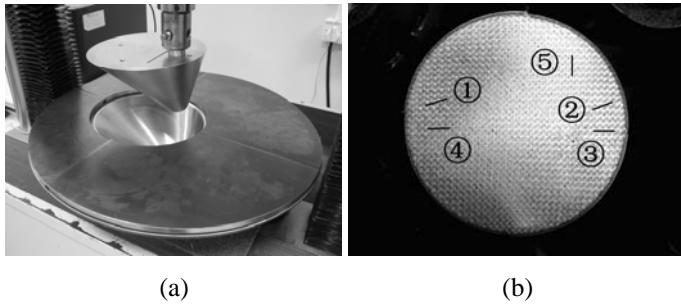


Fig. 1. Stamping set-up: (a) equipment; (b) sample orientation

There were totally 5 channels of sensors attached on different locations of the sample surface, as illustrated by figure 1(b). The obtained shear angle history is plotted in figure 2, where the square dots represent corresponding angles directly measured on the specimen after stamping finishes. The difference between the shear angle by the sensor and direct measurement is about 10%. Sensors of channel ③ and ⑤ breaks in the middle of the test due to the excessive off-angle and shear deformation; yet, their extended tendencies approximately go through the directly measured results.

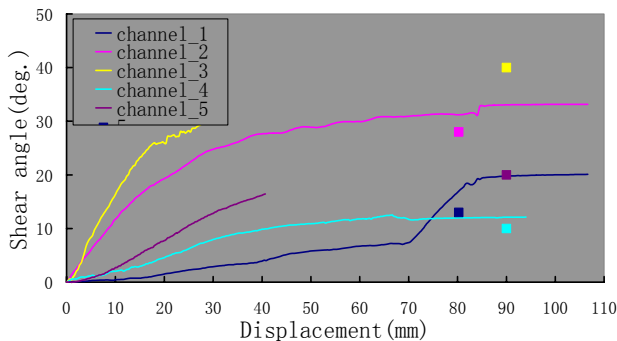


Fig. 2. Measured shear angle by sensors

The evolution of shear angle reveals that the shear of

textile composite sheet has a nonlinearly decreasing history under a constant stamping speed. Furthermore, the shear distribution on the finally stamped sample is dependent on both contour slope of the mould and initial yarn orientation. Figure 3 schematically demonstrates the shear distribution on the eccentric cone contour from the top view, where lighter regions have smaller shear while darker regions have larger shear. It is clearly seen that the white belts along the initial yarn directions almost do not deform, and significant shear is located in the regions along 45° to the yarns. On the other hand, since the slope at the right flank of mould is larger than that at the left, the largest shear angle occurs at the middle right part. It is also obvious that the deformation increases from undeformed bottom region to the edge of the contour. All these results are in accordance with our empirical expectations.

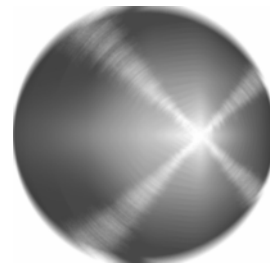


Fig. 3. Schematic shear distribution on the stamped sample

3.2 Measurement of wrinkling

Direct measurements of strain were made on the stamped sample in a more precise way, so as to verify the previously proposed theoretical model of failure [7]. The wrinkling criterion is expressed as a relationship between forces and stresses, which is not convenient to measure during real stamping operation. Hence, the criterion should be first transferred to strain relations. Considering two decoupled groups of yarns, 1 and 2, and neglecting the energy dissipated by rotary and sliding friction for the present specimen at room temperature, the criterion for wrinkling reduces to a simplified form:

$$E \cdot \cos \gamma \cdot \left[\frac{4I}{D} + \frac{n\pi D^2 w_0 (\varepsilon_1 + \varepsilon_2)}{16} \right] \leq 2w_0 \sin \gamma \cdot \bar{P}(\gamma) \quad (1)$$

where $E = 10.5\text{GPa}$ is yarn tensile modulus; $EI = 2.4 \times 10^{-7}\text{Nm}^2$ represents the bending property of a yarn; \bar{P} is the transversely compressive force between yarns in a fabric cell; $w_0 = 4.34\text{mm}$ is the initial yarn width; $D = 18\mu\text{m}$ is fiber diameter; $n = 4943$ is the number of fibers in a yarn; ε and γ are

measured tensile strain and shear angle along yarns, respectively. Introducing a virtual wrinkling energy W_v , which is equal to the left part minus right part in equation (1), then

$$\begin{cases} W_v < 0 & \text{(wrinkling happens)} \\ W_v > 0 & \text{(wrinkling does not happen)} \\ W_v = 0 & \text{(critical state)} \end{cases} \quad (2)$$

In equation (1), the coefficient of term $(\varepsilon_1 + \varepsilon_2)$ is extremely large compared with the others, it means even a small error in the tensile strain measurement has significant influence in calculating W_v . To reduce this error, we neglect the longitudinal strain along yarns and only consider the shear. The results are plotted in figure 4, where the dots in dashed square boxes indicate observed wrinkling on the stamped sample by eyes, and the onset of wrinkling can be determined by a negative virtual energy. The absolute value of W_v indicates how far the deformation is away from the critical wrinkling state.

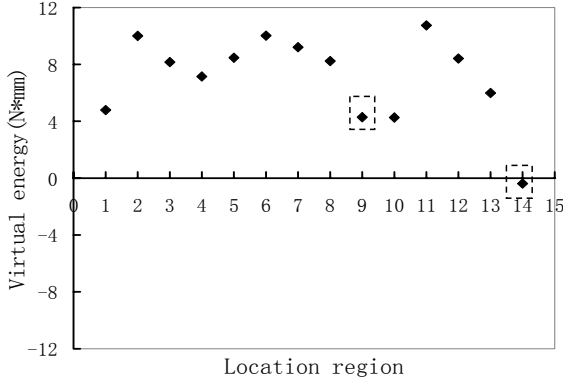


Fig. 4. Virtual wrinkling energies at different locations

It shows that the predicted wrinkling from the theoretical criterion is consistent with the observed phenomena after stamping except for only one location of disagreement. From another point view, the validity of the theoretical model of wrinkling can be considered up to about 93% in comparison to the real stamping experiments.

4 EVALUATION AND OPTIMIZATION OF STAMPING OPERATION

4.1 Mould shape and initial sample orientation

To make it simplified, the shear distribution of the woven fabric will be estimated through two decoupled terms: mould shape, C , and sample orientation, $G(x, y)$. Previous research shows that for many different contours, the yarn directions after

stamping approximately remain orthogonal and unchanged from the top view, which can be a basic assumption. Then for a general contour surface $f(x, y, z) = 0$, the distribution of shear angle of a balanced woven fabric after stamping is estimated as

$$\begin{cases} \gamma(x, y) = C \cdot G(x, y) \\ C = \frac{\pi}{2} - 2 \arcsin \sqrt{\frac{1}{4k_1^2(x, y) + 4} + \frac{1}{4k_2^2(x, y) + 4}} \\ G(x, y) = \sin 2\alpha \end{cases} \quad (3)$$

where k_1 and k_2 are the slopes of current point along two yarn directions on mould surface, respectively; α is the angle between yarns and the horizontal tangential direction of current point (see figure 5).

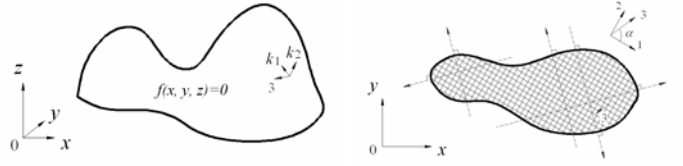


Fig. 5. A general mould and a general sample orientation

Therefore, the principle to avoid wrinkling is,

$$\max[\gamma(x, y)] < \gamma_c \quad (4)$$

where γ_c is the critical shear angle at wrinkling by the theoretical prediction.

4.2 Blank holder force

From an energy point of view, in order to make the material sufficiently sheared without breakage of yarn, the work done by the material's sliding friction beneath the blank holder should be larger than corresponding shear energy but smaller than yarn breaking energy. Therefore, the force per unit fabric cell exerted by the blank holder, $\bar{F}(x, y)$, should satisfy

$$\begin{cases} \mu_b \bar{F}(x, y) \cdot w_0^2 \cdot w_0 [\cos(\frac{\pi}{4} - \frac{\gamma_c}{2}) - \frac{1}{\sqrt{2}}] > \\ w_0 \cdot \gamma_c \cdot [\mu N(1 + \frac{3\gamma_c}{2\pi}) \sqrt{\frac{\cos \gamma_c}{\pi}} + 2\bar{P}(\gamma_c) \sin \gamma_c + 2\mu \bar{P}(\gamma_c) \cos \gamma_c] \Rightarrow \\ \mu_b \bar{F}(x, y) \cdot w_0^2 < \bar{\sigma}_e \cdot A \end{cases}$$

$$\frac{\gamma_c \cdot [\mu N(1 + \frac{3\gamma_c}{2\pi}) \sqrt{\frac{\cos \gamma_c}{\pi}} + 2\bar{P}(\gamma_c) \sin \gamma_c + 2\mu \bar{P}(\gamma_c) \cos \gamma_c]}{w_0^2 \cdot [\cos(\frac{\pi}{4} - \frac{\gamma_c}{2}) - \frac{1}{\sqrt{2}}]} < \mu_b \bar{F}(x, y) < \frac{\bar{\sigma}_e \cdot A}{w_0^2} \quad (5)$$

where μ_b is the sample's sliding frictional coefficient under the blank holder; $\bar{\sigma}_e$ is the average elastic limit of a single yarn; A is the yarn cross-sectional area. Considering the specific values for the present

specimen, the suitable range for the blank holder force is $1.2\text{N} < \mu_b \bar{F}(x, y) < 75\text{N}$.

5 TECHNICAL RECOMMENDATION

A diagram can be established to evaluate the formability of the balanced plain woven textile composite preforms during stamping operation. In most cases, the energy dissipated by rotary friction can be neglected, then, the critical shear angle at wrinkling is deduced as a function of the material properties:

$$\begin{cases} \gamma_c = \arccos \frac{1}{\sqrt{(2A - \mu)^2 + 1}} \\ A(\gamma) = \frac{1}{\bar{P}(\gamma)} \left(\frac{EI}{Dw_0} + \frac{\sum F}{16} \right) \end{cases} \quad (6)$$

A prediction of wrinkling after stamping is explicitly illustrated by figure 6. The black curve in the left coordinate indicates the critical shear angle at wrinkling varying with material properties, while the blue curves in the right coordinate are the shear angles required to conform to the mould. For a given mould, a blue curve can be determined in figure 6 (e.g., $C = 1.4$). To prevent wrinkling, material properties of the textile sample should be selected so that the point on the black curve locates over the whole blue curve of $C = 1.4$ (e.g., if $2A - \mu = 18$). On the contrary, if $2A - \mu = 4$, a horizontal line can be drawn from O' to intersect with the blue curve; in this case, on the location with an orientation of $\alpha > 0.57$, wrinkling will happen. On the other hand, for given material properties (e.g., $2A - \mu = 4$), if the combination of mould shape and orientation locates in the red region, wrinkling occurs; and locating in the green region indicates no wrinkling. By this diagram, we can conveniently predict the wrinkling failure of a woven textile composite preform, evaluate the material's formability, and optimize the mould shape and blank sheet orientation.

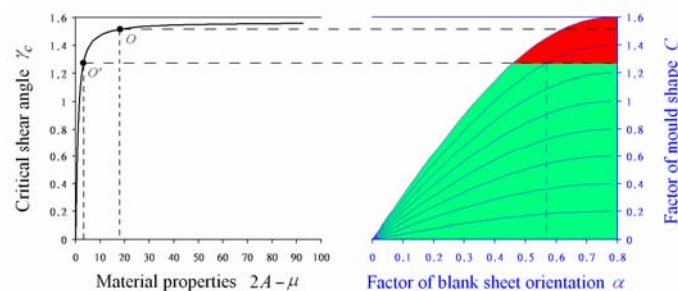


Fig. 6. Illustration of material's formability during stamping

6 CONCLUSIONS

This paper discusses stamping tests on woven textile composite preforms. By measurement of conductive fiber sensor, the shear distribution and evolution of the sample during stamping were acquired. The validity of a previously proposed criterion for wrinkling was evaluated, achieving more than 90% of agreement with the experiments. Quantitative estimations and optimizations were carried out for the mould shape, blank sheet orientation, and blank holder force. To facilitate the understanding and use of practical engineers, the formability of woven fabric composite preforms in stamping operation is explicitly illustrated, which can be referred to in practical applications.

ACKNOWLEDGEMENTS

The work reported in this paper is a part of a Hong Kong CERG project numbered HKUST6012/02E. The financial support from the Hong Kong Research Grant Council is gratefully acknowledged. The authors would also like to thank the Benchmark group led by Prof. J. Cao of Northwestern University, USA, for supplying the composite materials.

REFERENCES

1. Lim T.C. and Ramakrishna S., 'Modeling of Composite Sheet Forming: A Review', *Composites Part A*, 33, (2002) 515-37
2. Lee J.H. and Vogel J.H., 'An Investigation of the Formability of Long Fiber Thermoplastic Composite Sheets', *Journal of Engineering Materials and Technology*, 117, (1995) 127-32
3. Wang J., Paton R. and Page. J.R., 'The draping of woven fabric preforms and prepregs for production of polymer composites', *Composites Part A*, 30, (1999) 757-65
4. Chung S.Y. and Swift H.W., 'An Experimental Investigation of Redrawing of Cylindrical Cups', In: *Proc. Institution of Mechanical Engineers*, (1951) 199-211.
5. Prodromou A.G. and Chen J., 'On the Relationship between Shear Angle and Wrinkling of Textile Composite Preforms', *Composites Part A*, 28, (1997) 491-503
6. Long A., Robitaille F., Souter B. and Rudd C., 'Permeability Prediction for Sheared, Compacted Textiles during Liquid Composite Moulding', In: *Proc. 13th International Conference on Composite Materials*, Beijing, China, (2001) 636.
7. Zhu B., Yu T.X., Teng J. and Tao X.M., 'Theoretical Modeling of Large Shear Deformation and Wrinkling of Plain Woven Composite', Accepted by *Journal of Composite Materials*, (2007)
8. Zhang H., Tao X.M., Yu T.X. and Wang S.Y., 'Conductive Knitted Fabric as Large-strain Gauge under High Temperature', *Sensors Actuators A*, 126, (2006) 129-40